

Investigation of the Metal-Insulator Transition in V_2O_3 by Nuclear Magnetic Resonance

MARK RUBINSTEIN

Naval Research Laboratory, Washington, D. C. 20390

(Received 13 March 1970)

The metal-to-insulator phase transitions have been investigated in Cr- and Al-doped V_2O_3 by nuclear magnetic resonance. Two distinct transitions exist in this system: a low-temperature antiferromagnetic insulator-metal transition, and a high-temperature metal-insulator transition. An abrupt change in the Knight shift is noted at the high-temperature transition, while the resonance signal completely vanishes in the low-temperature antiferromagnetic phase. A theoretical model is developed which explains the existence of both transitions, and the anomalous properties of the metallic state. The magnitude of the magnetic moment in the antiferromagnetically ordered state is discussed.

I. INTRODUCTION

The compound V_2O_3 exhibits several unusual phenomena, and has been extensively investigated in recent years. At room temperature it is a fairly good metal, with the purest samples showing resistivities on the order of $10^{-3} \Omega \text{ cm}$. In the metallic state, the temperature dependence of the magnetic susceptibility χ is anomalous^{1,2} (for a metal), with $\chi = \text{const} + C/(T + \theta)$. When the temperature is decreased below 150°K , V_2O_3 undergoes a first-order phase transition from the metallic state to an insulating state, with an accompanying increase of resistivity measuring nearly seven orders of magnitude.³ Associated with the metal-insulator transition is a change in crystal structure from the high-temperature corundum structure with rhombohedral symmetry to a low-temperature monoclinic symmetry phase.⁴ There is a volume expansion of 3.5% as V_2O_3 is cooled through the transition temperature. Below the transition V_2O_3 is an antiferromagnet with a moment of $\sim 1.2 \mu_B$ per V atom.⁵

In addition to the metal-to-insulator transition at $\sim 150^\circ\text{K}$, there is an anomalous change in conductivity in the temperature region $400\text{--}600^\circ\text{K}$.^{6,7} This anomaly has been shown to be associated with a gradual change from metallic to insulating behavior, in which the high-temperature phase ($> 600^\circ\text{K}$) is an insulator.⁸ Both phases of this high-temperature transition have the corundum crystal symmetry, but a marked change in the c/a ratio accompanies the transition.

Mott⁹ has predicted that an abrupt metal-insulator, itinerant-electron-localized-electron transition will occur when the interionic separation is forced to pass through critical value. Since each of the two resistance anomalies in V_2O_3 is accompanied by an anomaly in the thermal expansion, it would appear that they may both be metal-to-insulator transitions of the type envisioned by Mott.

The basis for the ideas that the V_2O_3 transitions are Mott-type transitions is contained in a recent series of papers by McWhan, Rice, and Remeika.^{8,10,11} These authors studied the resistivity and the lattice distortion of V_2O_3 as a function of pressure, temperature,

chromium doping, and titanium doping. The results of their efforts are summarized in a generalized phase diagram for the system reproduced in Fig. 1. There are three distinct phases in this system: the metallic (M) phase, the insulating (I) phase, and the antiferromagnetic insulating (AF) phase. At room temperature and atmospheric pressure, pure V_2O_3 is situated in the metallic phase. As the temperature is lowered, the undoped material passes through the M-AF phase boundary at $\sim 160^\circ\text{K}$. Conversely, as the temperature is raised, pure V_2O_3 appears to pass through the extension of the M-I phase boundary at $\sim 550^\circ\text{K}$. How-

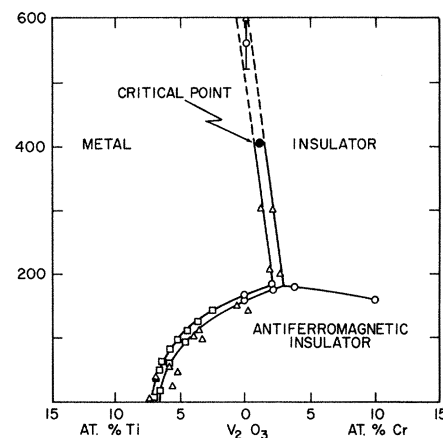


Fig. 1. Phase diagram of Cr- and Ti-doped V_2O_3 (Ref. 8).

ever, the M-I phase boundary terminates at a critical point, so that the high-temperature transition in pure V_2O_3 reflects supercritical behavior. The phase transition is no longer a well-defined, abrupt, first-order transition, but is a gradual change from metallic to insulating behavior. When a small percentage of chromium ions is substituted for vanadium in V_2O_3 , a definite first-order phase transition between the metallic and insulating phases may exist, with the transition temperature rapidly decreasing as a function of Cr doping. At a critical concentration, near 3% Cr, the M-I

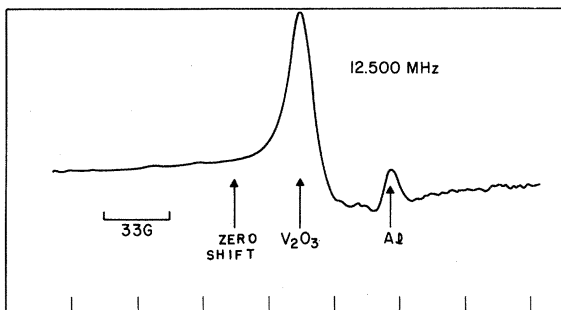


FIG. 2. Room-temperature trace of the ^{51}V NMR signal in powdered V_2O_5 . The positions of the reference NaVO_3 line and the extraneous Al line are also indicated.

transition temperature and the M-AF transition temperature are equal ($\sim 160^\circ\text{K}$). For chromium dopings greater than 3% an intermediate metallic state does not exist, and the only observed transition is a direct I-AF transition (at atmospheric pressure). The double lines in the phase diagram represent hysteretic behavior.

In the case of V_2O_5 , there are at least ten opposing views to the Mott transition model of McWhan, Rice, and Remeika. The author has adopted the conclusions of McWhan *et al.* as a point of departure, but the reader is advised that this is a subject of intense scientific controversy.

In this paper, we are reporting on a study of the ^{51}V nuclear magnetic resonance in pure and Al- or Cr-doped V_2O_5 as a function of temperature, with special attention paid to the crossing of the phase boundaries. Our results tend to substantiate the findings of McWhan, Rice, and Remeika,⁸ with one exception. We find, contrary to the above authors, that the M-I phase boundary is not sharp and uniform below the critical point, but corresponds to an inhomogeneous transition. Different regions of the Cr-doped samples undergo their respective phase transitions at different temperatures, corresponding to the random placement of the impurity ions in the crystal. On the other hand, we find the M-AF transition to be sharply defined, even when the percentage of Cr doping (or Al doping) is quite large.

II. EXPERIMENTAL

We are reporting on the observation and study of the ^{51}V nuclear resonance signal in the mixed oxide system $(\text{V}_{1-x}\text{Cr}_x)_2\text{O}_5$ and $(\text{V}_{1-x}\text{Al}_x)_2\text{O}_5$, where x is varied from 0 to 0.08. The samples were prepared following a prescription described by MacMillan.¹² Fisher certified 99.9% V_2O_5 powder was mixed with the appropriate proportions of Al_2O_3 or Cr_2O_3 powder, and pressed into pellets. The samples were then fired in hydrogen at 1350°C for 24 h. The ^{51}V nuclear resonance spectra were obtained using a Varian 4200 wide-line NMR spectrometer at a fixed frequency of 12.5 MHz. Variable sample temperatures were obtained with a flowing gas system. Temperatures were measured with a copper-

constantan thermocouple placed within the flowing gas stream.

The room-temperature ^{51}V NMR spectrum of pure V_2O_5 in the metallic state is shown in Fig. 2. The additional resonance on the high-field side of the V signal is due to the aluminum in the NMR probe. The Knight shift was measured with respect to a water solution containing a small amount of dissolved NaVO_3 , and the position of zero Knight shift is also indicated in Fig. 2. The ^{51}V NMR of pure V_2O_5 was measured as a function of temperature from 160 to 420°K . In the range studied, our results are in agreement with the previous measurements of Jones,¹ who performed measurements up to 575°K using single crystals which were ground into a powder to allow penetration of the rf field into the metal. The Knight shift was found to vary from -0.61% at 175°K to $+0.1\%$ at 575°K . Jones also measured the susceptibility χ of a single crystal of V_2O_5 in the temperature range 175 – 300°K , and plotted the Knight shift as a function of susceptibility with temperature the implicit variable. The Knight shift and the susceptibility were found to vary in a linear manner and Jones was able to disentangle the temperature-dependent and the temperature-independent contributions to both the susceptibility and the NMR resonance field. The two principal contributions to the susceptibility are the temperature-dependent d -band paramagnetism $\chi_d(T)$, and the temperature-independent orbital paramagnetism χ_{VV} , which is the analog in metals of the Van Vleck paramagnetic susceptibility. The total susceptibility at a temperature T is given by (ignoring a small diamagnetic correction)

$$\chi(T) = \chi_d(T) + \chi_{\text{VV}}. \quad (2.1)$$

Jones deduced for V_2O_5

$$\chi_{\text{VV}} = 210 \times 10^{-6} \text{ emu/mole}, \quad (2.2)$$

$$\chi_d(T) = C/(T + \theta), \quad (2.3)$$

with $C = 0.657$ (emu/mole) $^\circ\text{K}$ and $\theta = 600^\circ\text{K}$. This large temperature-dependent susceptibility is anomalous for a metal, and its implications will be discussed later.

The ^{51}V NMR field shift also consists of two contributions: a temperature-dependent shift $(\Delta H/H)_d$ resulting from hyperfine interactions of the form $AI\langle S \rangle$, where the temperature dependence is contained in the time-averaged electron spin $\langle S \rangle$, proportional to $\chi_d(T)$, and a temperature-independent field shift $(\Delta H/H)_{\text{VV}}$ arising from the field-induced Van Vleck paramagnetism, proportional to χ_{VV} .

The total shift $\Delta H/H$ is written as

$$(\Delta H/H) = (\Delta H/H)_d + (\Delta H/H)_{\text{VV}}, \quad (2.4)$$

$$(\Delta H/H) = \alpha_d \chi_d(T) + \beta' \chi_{\text{VV}}. \quad (2.5)$$

Jones gives

$$\alpha_d = -140 \times 10^3, \quad \beta' = +395 \times 10^3. \quad (2.6)$$

The Knight shift, like the susceptibility, is strongly temperature dependent and actually changes sign from a negative to a positive value as the temperature is increased owing to the two opposing contributions.

The addition of Cr or Al ions as substitutional impurities in V_2O_3 produces a marked change in the ^{51}V NMR spectra. In addition to the primary resonance line observed by Jones in pure V_2O_3 a secondary line appears, displaced from the primary by a significant amount to a less negative value of the Knight shift. Increasing either the impurity concentration or the temperature causes the secondary line to increase in intensity, and the primary line to decrease. These two effects are shown in Figs. 3 and 4.

In Fig. 3 are reproduced room-temperature spectra of the V nuclear resonance signal in V_2O_3 samples containing 0, 1, 2, 4, and 8 at. % chromium ions, respectively. The $23^\circ C$ spectra of pure V_2O_3 consists of a single line which is displaced from a ^{51}V reference line by -0.31% . With the addition of 1% Cr the amplitude of the primary line is reduced, and a secondary line appears at a Knight-shift displacement of -0.05% . Again the signal on the high-field side of the primary

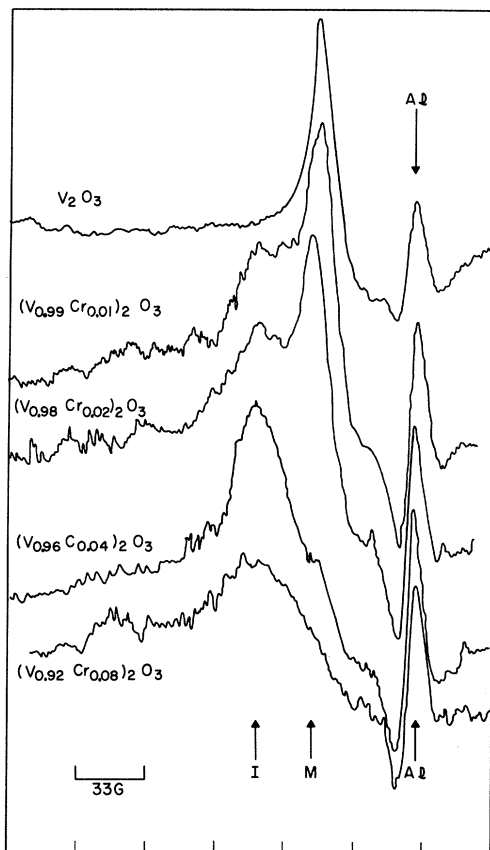


FIG. 3. Room-temperature spectra of the ^{51}V NMR signal $(V_{1-x}Cr_x)_2O_3$. The positions of the metallic-phase and insulating-phase resonance lines are indicated by arrows. The Al resonance signal originates in the Al NMR probe.

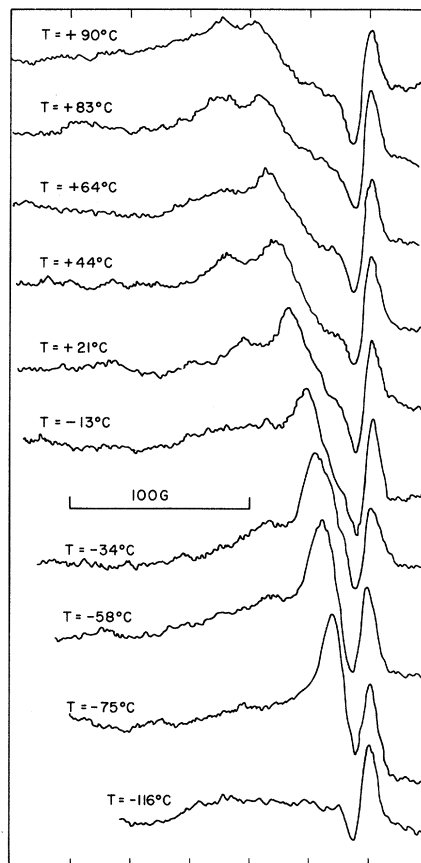


FIG. 4. Temperature dependence of the ^{51}V NMR spectra in $(V_{0.98}Cr_{0.02})_2O_3$. The applied magnetic field increases from left to right. The spectrometer frequency is set at 12.500 MHz. The resonance line at the extreme right, unaffected by changes in the sample temperature, is extraneous, and originates in the Al NMR probe.

line is an extraneous resonance due to the aluminum probe. In the 2% Cr sample, the amplitude of the secondary line has increased at the expense of the primary line; and in the 4% Cr sample only the barest trace of the primary line remains. The spectrum of $(V_{0.92}Cr_{0.08})_2O_3$ contains only the secondary resonance line.

The dependence of the resonance spectrum on temperature is shown in Fig. 4 for a $(V_{0.98}Cr_{0.02})_2O_3$ sample. At the lowest temperature ($T = -116^\circ C$), only the spurious aluminum probe resonance is observed. At this low temperature, the sample is antiferromagnetic and the V resonance is displaced to a very high frequency by the large nuclear hyperfine field present in the ordered state, and is not observed. In fact, it was the abrupt disappearance of the NMR signal which provided the first experimental evidence for the antiferromagnetic ordering of V_2O_3 .¹

At temperatures somewhat higher than the transition temperature (e.g., $T = -75^\circ C$), a single ^{51}V line appears which is indistinguishable (except for a slight increase

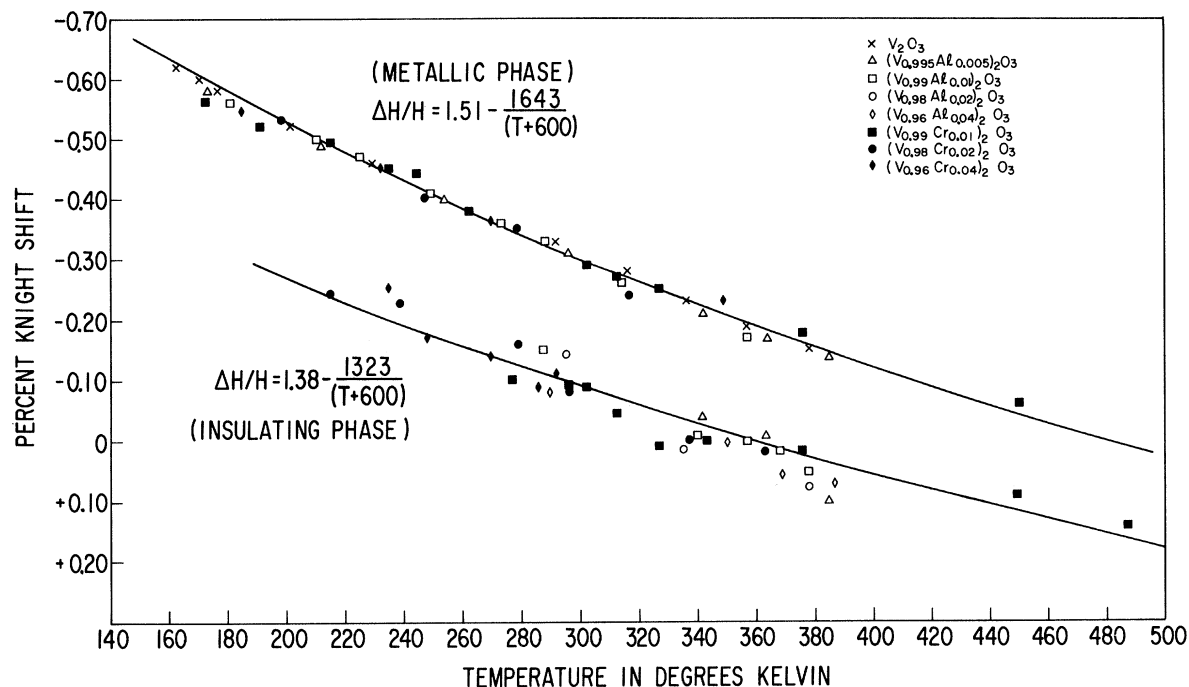


FIG. 5. Temperature dependence of the $(V_{1-x}Cr_x)_2O_3$ and $(V_{1-x}Al_x)_2O_3$ Knight shifts in both the metallic and insulating phases. The insensitivity of the Knight shift to the impurity type or concentration indicates the presence of two distinct phases in the system.

in linewidth) from the resonance line in pure V_2O_3 . At still higher temperatures, the secondary line appears in the spectrum, drawing its intensity from the primary resonance line. The positions of both lines are strongly temperature dependent, the secondary line shifting with temperature somewhat less rapidly than the primary line. At the highest temperature shown in the figure ($T = +90^\circ C$) the secondary line is slightly more intense than the primary line. At still higher temperatures the secondary line continues to gain in amplitude, and the primary line to diminish, until at $T \approx +200^\circ C$ only the secondary line can be observed for the 2% Cr sample. Above this temperature the secondary resonance ceases to grow in intensity as the temperature is increased, and ultimately decreases in the usual manner, inversely proportional to the absolute temperature. For samples with greater Cr concentrations, the temperature at which the primary and secondary resonance intensities are comparable, is lower. For $(V_{0.92}Cr_{0.08})_2O_3$ only the secondary resonance line is observed above the antiferromagnetic transition. Nearly identical behavior is observed in the Al-doped samples.

In Fig. 5 we show the temperature dependence of the Knight shifts for both the primary and secondary resonance line in a composite plot of data for the $(V_{1-x}Cr_x)_2O_3$ and $(V_{1-x}Al)_2O_3$ system. Jones's empirical expression for the Knight shift of pure metallic V_2O_3 , expressed in percent, $\Delta H/H = 1.51 - 1643/(T + 600^\circ K)$, is plotted as the solid line labeled "metallic phase."

The dramatic changes of the resonance spectra of V_2O_3 with temperature or impurity concentration constitute highly unusual behavior for a metallic alloy. The appearance of satellite lines on the wings of the central resonance line has been noted many times before in other metals and is caused by the perturbing effect of the impurity ion on the neighboring host nuclei. However, in no other system has the ratio of the central line intensity to the satellite line intensity been so extremely temperature dependent.

This behavior may be understood by assuming that the metallic (M) and insulating (I) phases of V_2O_3 coexist over a limited temperature range. The primary resonance line is assigned to nuclei within the metallic regions, and the secondary line is assigned to nuclei existing within the insulating regions of the crystal. Pure V_2O_3 undergoes a gradual (supercritical) phase transition from a metal to an insulator at $\sim 300^\circ C$. The effect of Cr impurities is to precipitate the phase transition at a lower temperature. V^{3+} ions in Cr-rich regions or near a Cr impurity undergo the M-I phase transition first; at a higher temperature V ions which are further from the impurity pass through the phase boundary, etc. Ultimately, the entire crystal is in the insulating state.

The Mott transition from the metallic to the insulating state involves a change in the $3d$ electrons from an itinerant to a localized nature.⁸ This change in the nature of the $3d$ wave function surrounding a V nucleus

will result in a corresponding change in the ^{51}V Knight shift as the transition is passed. Thus, the primary resonance line and the secondary resonance line, corresponding to the metallic and insulating phases, respectively, will occur at somewhat different magnetic fields. As more and more of the crystal is converted from a metallic to an insulating phase, the intensity of the primary resonance will diminish.

At any given V ion in Cr- or Al-doped V_2O_3 , the transition is abrupt. There are only two resonance lines, an M-phase line and an I-phase line. If the transition were continuous, resonances would be observed at fields intermediate between the I phase and the M-phase lines. What is a continuous function of temperature is the relative distribution of insulating and metallic phases in the material.

We may construct an "NMR phase diagram" of the $(\text{V}_{1-x}\text{Cr}_x)_2\text{O}_3$ system by (somewhat arbitrarily) choosing as the M-I transition temperature, the temperature at which the "metallic" primary resonance line is equal in intensity to the "insulating" secondary resonance line. For the M-AF (or I-AF) transition temperature, we choose that temperature at which the resonance signal vanishes. The resulting diagram is shown in Fig. 6. We note that this diagram is very similar to the phase diagram of Fig. 1, which was deduced by McWhan *et al.*⁸ from the occurrence of the resistance anomalies. The occurrence of hysteresis is indicated by the shaded portions. We disagree with the implication found in Ref. 8 that the M-I transition is an abrupt one. Rather, the gradual evolution in the NMR spectra of a pure "metallic" resonance into a pure "insulator" resonance leads us to conclude that the transition is broad and inhomogeneous. However, the main conclusions of Ref. 8 remain unaltered.

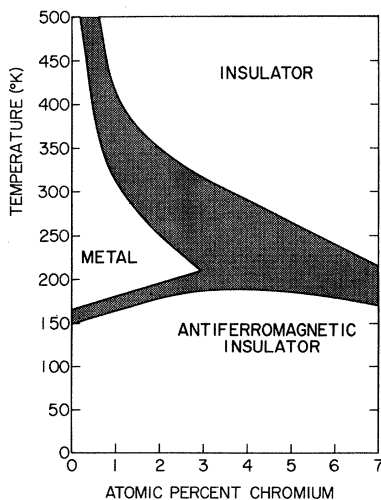


FIG. 6. Phase diagram of Cr-doped V_2O_3 , as determined from NMR measurements. The shaded portion indicates the regions of hysteresis, and a simultaneous coexistence of phases.

III. METALLIC STATE

The theory of the Mott transition is based on the concept of a critical interatomic spacing a_c . When the interatomic distance $a > a_c$, the outermost electrons are localized around each atomic site, bound there by the ionic potential. If the lattice is now contracted (e.g., by the application of pressure) to the point that $a = a_c$, the outermost electrons suddenly become itinerant; an abrupt transition is made from a localized insulator to a band metal. Since a change in the lattice constant accompanies both the high- and low-temperature metal-insulator transitions in V_2O_3 , it would appear that V_2O_3 is a good candidate for a Mott-transition material. However, the simplest theory of the Mott transition¹⁸ is not in accord with the known facts concerning the metal-insulator transition in V_2O_3 .

Following Mott's not-very-recent paper, assume that the lattice parameter is slightly greater than the critical interatomic distance, so the system is an insulator at absolute zero. Let E_m and E_i be the energies per electron at $T=0$ of the metallic and insulating states with $E_m > E_i$. The free energy of the metallic state at temperature T is written

$$\Phi_m(T) = E_m - TS_m = E_m - \pi^2 k^2 T^2 / 2E_F, \quad (3.1)$$

where S_m is the entropy of the metallic phase, and E_F the Fermi energy. If we assume the free energy of the insulating state does not vary appreciably with temperature, a M-I phase transition will occur at a critical temperature T_c such that $\Phi_m = \Phi_i$; i.e.,

$$\pi^2 k^2 T_c^2 / 2E_F = E_m - E_i. \quad (3.2)$$

Mott's simple theory, therefore, places the insulator as the low-temperature phase and the metal as the high-temperature phase, whereas the reverse is observed in the M-I transition of V_2O_3 .

A clue to the missing element in the theory is provided by the anomalous temperature dependence of the Knight shift and the magnetic susceptibility in the metallic state. V_2O_3 possesses a susceptibility which is strongly temperature dependent at quite moderate temperatures. Most metals, on the other hand, display Pauli temperature-independent susceptibility, in which the susceptibility deviates from its absolute-zero value only when the temperature is of the order of the Fermi energy. Labbe¹⁴ has shown, however, that if a singularity in the density of states exists in the vicinity of the Fermi level, large and strongly temperature-dependent Pauli susceptibility can result.

Van Hove¹⁵ was the first to investigate the nature of these critical points in the density of states, and to show that their existence was a necessary result of the lattice periodicity. These Van Hove singularities consist of several types. A one-dimensional crystal contains infinities at the extreme frequencies of each branch. This was the type of singularity investigated by Labbe and Friedel^{14,16} to explain the anomalous properties of V_3Si .

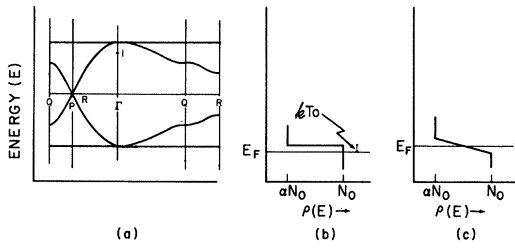


FIG. 7. (a) Energy-level diagram of the two-dimensional V_2O_3 band structure (Ref. 18). Only the lowest band is occupied. The Fermi energy touches this band at the twofold degenerate Γ point. (b) Density of states near the Fermi energy. The Fermi level is displaced by kT_0 below the discontinuity, presumably by lack of stoichiometry. (c) "Rounded" density of states near the Fermi energy. The discontinuity at the Fermi level is smeared by an energy kT_0 because of the finite lifetime of the conduction electrons.

A two-dimensional crystal will contain discontinuities and/or logarithmic infinities, while a three-dimensional crystal contains critical points through which the density of states remains continuous, while a discontinuity appears in its derivative. The possibility of a logarithmic infinity in a three-dimensional crystal has been investigated recently by Gilat,¹⁷ who concluded that such a singularity may exist, provided the band degeneracy is large enough.

A band-structure calculation of V_2O_3 has recently been published by Nebenzahl and Weger¹⁸ from which the nature and energy of these singularities may be determined. These authors utilize tight-binding wave functions composed of the triply degenerate t_{2g} levels of the cubic field, split by the trigonal field distortion into a singlet and a doublet¹⁹ with the singlet lying lowest. (The assumed disposition of the singlet and doublet levels in V_2O_3 is opposed²⁰ to that found in $Al_2O_3:V^{3+}$.) Nebenzahl and Weger then assume that the singlet functions will form their bands corresponding to bonding and antibonding states of pairs of electrons localized on c -axis neighboring sites, with one electron per V ion taking part. The doublet functions form four two-dimensional bands in the basal plane. The band structure derived from these wave functions is reproduced in Fig. 7. Each of the four bands has space for two electrons per unit cell (with spin up or down). Since there are two electrons per unit cell to be put into the bands, only one band is filled and three remain empty. It is seen that the top of the filled band lies at the Γ point of the Brillouin zone and is degenerate with another higher-lying band at that point. V_2O_3 is thus semimetallic above the Néel point. We define m_v as the effective mass of the valence band and m_c the effective mass of the higher-lying conduction band. The density of states ρ near the Γ point ($k=0$) is given by

$$\rho = \frac{dN}{dk} \bigg/ \frac{dE}{dk} = \frac{m}{2\pi\hbar^2} \quad (3.3)$$

for a two-dimensional band, where N is the number of states per unit volume. The Van Hove singularity at the Γ point is seen to be a discontinuity of magnitude $(m_v - m_c)/(2\pi\hbar^2)$. The density of states near the Γ point is also shown in Fig. 7. We now assume that the Fermi level at $T=0$ is just slightly below the discontinuity by an amount kT_0 rather than coincident with it. This may be a result of lack of complete stoichiometry. With this model it is possible to understand the temperature dependence of the V_2O_3 susceptibility. The paramagnetic susceptibility becomes temperature dependent when $T \sim T_0$, where T_0 is the degeneracy temperature $\approx 100^\circ\text{K}$; in a normal metal the susceptibility becomes temperature dependent only when $T \sim E_F/k$, a much higher temperature. The detailed theory describing the effects of the proximity of the Fermi level to a Van Hove discontinuity is given by Cohen, Cody, and Halloran²¹ in their discussion of the normal-state properties of β -tungsten superconductors. The paramagnetic susceptibility $\chi(T)$ is given by the expression

$$\chi(T) = \mu_B^2(1-\alpha)N_0F_\alpha(T) + \chi_{VV}, \quad (3.4)$$

where

$$N_0(1-\alpha) = (m_v - m_c)/(2\pi\hbar^2),$$

$$F_\alpha(T) = \{1 + \exp[-E_F(T)/kT]\}^{-1},$$

the value of the Fermi function at the band edge, and α is a dimensionless parameter indicating the fractional change of density of states at the discontinuity. The resulting susceptibility is temperature independent for $T \ll T_0$ and varies inversely with temperature for $T \gg T_0$. As Cohen *et al.* point out, the first term on the right-hand side of Eq. (3.4) should be multiplied by $[1 + N_0J(1 - \frac{1}{2}\alpha F_\alpha(T))]^{-1}$ to take into account the diminishment of χ by the antiferromagnetic exchange interaction J . At high temperatures, this has the effect of replacing T by $(T + \theta)$. If we further assume that $m_c \gg m_v$, the resulting expression for χ in the limit $(T + \theta) \gg T_0$ will reduce to Jones's expression $\chi_a(T) = C/(T + \theta)$. [An alternative treatment of the Van Hove discontinuity is sketched in Fig. 7(c). Here, the Fermi energy lies exactly on top of the discontinuity; however the discontinuity is slightly smeared by an amount kT_0 by electron-electron interactions. Although this model is a better one, we shall continue to use the model of Cohen *et al.*, since its results are worked out already.]

These same ideas can be used to explain the resistivity anomaly at $\sim 600^\circ\text{K}$ in pure V_2O_3 , which we have associated with the high-temperature M-I transition. Let ψ be the magnitude of a small lattice strain which changes the c/a ratio of V_2O_3 . The change in the lattice energy resulting from such a distortion is written as $+\frac{1}{2}B(T)\psi^2 + \dots$, where $B(T)$ is the temperature-dependent strain modulus. In the tight-binding approximation, the mutual overlap of the conduction-electron

wave functions varies exponentially with the interatomic distance, and the free energy of the electron-gas system will be a strong function of the strain. The electron-gas contribution to the strain energy has been shown by Labbe and Friedel¹⁶ to be of the form $-\frac{1}{2}A(T)\psi^2 + \dots$, where $A(T)$ is the electronic contribution to the strain modulus. Thus

$$E = -\frac{1}{2}[A(T) - B(T)]\psi^2 + \dots \quad (3.5)$$

Because of the motion of the Fermi level across the Van Hove discontinuity caused by increasing the temperature, the electron-gas modulus $A(T)$ will vary with temperature when the temperature is of the order of T_0 . When $A(T) = B(T)$, the lattice will spontaneously distort to a new configuration. This is commonly referred to as "softening" of the acoustic phonon mode. The lowering of the transition temperature with Al or Cr doping is due to local decrease in the value of B near the impurity, owing to a smaller ionic radii of these two ions with respect to V^{3+} . The detailed theory for the crystalline transformation of metals whose Fermi level is near a Van Hove discontinuity is worked out by Cohen *et al.*,²¹ who find

$$A(T) = CN_0U_2^2F_\alpha(T), \quad (3.6)$$

where N_0 is the density of states at $T=0$, U_2 is a deformation potential, C is a constant of order unity, and $F_\alpha(T)$ is the same function appearing in Eq. (2). The temperature dependence of the lattice contribution to the stress modulus is given by

$$B(T) \approx B(0) \exp(-2\gamma\beta T), \quad (3.7)$$

where γ is the Grüneisen constant and β is the thermal expansivity. At that temperature when $A(T) = B(T)$, an instability develops, and the lattice suddenly expands.²²

Experimentally, it is found that the c/a of V_2O_3 decreased by $\sim 1\%$ on passing through the 600°K M-I transition.⁸ The a -axis expansion results in a greater separation between V atoms in the basal plane. We propose that this small expansion is sufficient to cause the interatomic distance to pass the critical distance postulated by Mott as the boundary between metallic and insulating behavior. This is a speculation. The high-temperature transition is thus driven by the crystalline distortion, and the anomalous metallic susceptibility is seen to be a precursor to the M-I transition. The explanation for the low-temperature M-AF transition is somewhat different, being magneto-elastic in origin. We shall show later that this transition may actually be driven by the antiferromagnetic ordering of the crystal.

The essential feature of this model is that the Fermi energy and a Van Hove singularity nearly coincide. We have used the Nebenzahl-Weger band structure because it is the only detailed calculation available. Another band structure model for the corundum structure has

been proposed by Kleiner²³ and used by Honig and Reed²⁴ to explain the electrical properties of Ti_2O_3 . From group-theoretical arguments, Kleiner places the top of the valence band at the T point of the Brillouin zone, a point of fourfold degeneracy. The nature of the Van Hove singularity at that point has not been examined; it may be a cusplike critical point, or even a logarithmic infinity.¹⁷ Whatever its nature, it is believed that it will give rise to the effects similar to those discussed above. We believe that other models of the corundum band structure²⁵ which do not place the Fermi level near a Van Hove singularity are not applicable to V_2O_3 .

IV. INSULATING STATE

The M-I transition may be produced in one of two ways: by raising the temperature above $\sim 600^\circ\text{K}$, or by doping with Cr or Al impurities. According to the model we have proposed, the effect of doping is to alter the strain modulus B locally, reducing the temperature at which the Mott transition occurs.

Examination of the NMR spectra leads to the conclusion that the M-I transition is inhomogeneous in Al- and Cr-doped V_2O_3 , with insulating regions near the impurity sites (or in impurity-rich regions) coexisting with metallic regions, far from the impurity (or in impurity-poor regions) over a wide range of temperatures. The question arises as to whether such behavior is consistent with our current understanding of the Mott transition. Can, indeed, one speak of metallism as a microscopically local property? Or, is metallism strictly a bulk property, like long-range order, which a substance either has or has not? The author believes that the states involved can be more readily defined in terms of bonding (metallic or ionic) between neighboring atoms than in terms of bulk properties such as resistivity. However, the nuclear resonance spectra do not distinguish between the two types of metallisms.

The ground state of a free V^{3+} ion is $3d^2(^3F)$. Under a cubic ligand field the 3F state splits up into a degenerate orbital triplet 3T_1 lying lowest, with another triplet 3T_2 and a singlet 3A_2 lying successively above it. The effect of the trigonal field component and the spin-orbit coupling is to further split the ninefold (spin plus orbital) 3T_1 ground state. Following Abragam and Pryce,²⁶ it is convenient to introduce a fictitious orbital angular momentum l with the total value $l=1$ operating in the ground 3T_1 manifold. The real orbital angular momentum L is related to the fictitious quantity by the relation

$$\mathbf{L} = -\kappa\alpha\mathbf{l}. \quad (4.1)$$

α is an effective Lande factor which equals $\frac{3}{2}$ in the absence of 3P admixture into the 3F state and κ is the orbital reduction factor caused by covalent bonding to the oxygen ligands. The effective Hamiltonian representing the combined effect of the spin-orbit interaction

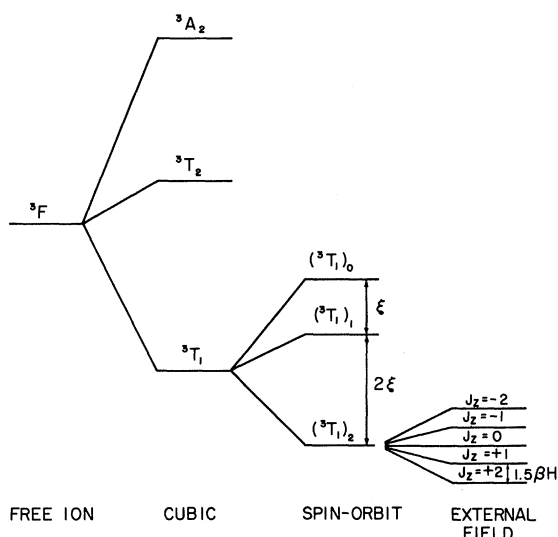


FIG. 8. Energy-level diagram of the V^{3+} ion in V_2O_3 .

and the trigonal ligand field on the ground 3T_1 state is²⁷

$$3\mathcal{C} = \Delta(1 - l_z^2) - \xi \mathbf{l} \cdot \mathbf{s}, \quad (4.2)$$

where Δ is the trigonal field splitting parameter and ξ is the effective spin-orbit coupling constant.

We now assert that the value $\Delta \approx 0$ ($\Delta < \xi$) is appropriate to the V^{3+} ion in V_2O_3 , notwithstanding the large value $\Delta \approx 1000 \text{ cm}^{-1}$ found in $Al_2O_3:V^{3+}$. The reasons for this choice are enumerated below.

(a) There is no detectable anisotropy in the Knight shift of the V_2O_3 NMR spectrum. A sizable value for Δ would result in a highly anisotropic NMR line shape, a doubly peaked powder pattern. A careful study showed no indication of anisotropic contributions to the NMR spectrum. This was previously pointed out by Jones.¹

(b) There is no observable quadrupole splitting in the NMR spectrum of V_2O_3 . A trigonal field gradient would produce a sizable nuclear quadrupole splitting in the ${}^{51}V$ nucleus ($I = \frac{7}{2}$) which is readily observed in other noncubic V compounds, e.g., VO_2 , V_2O_5 , and V_3Si .²⁸

(c) Jones reports that zero anisotropy was observed in single-crystal susceptibility measurements on V_2O_3 for various crystalline orientations with respect to the magnetic field. (See, however, Carr and Foner.²) A large value for the trigonal field parameter would result in highly anisotropic Van Vleck susceptibility.

It is not entirely unexpected that the trigonal crystal field in V_2O_3 will be different than that in $Al_2O_3:V^{3+}$. In going from ruby ($Al_2O_3:Cr^{3+}$) to Cr_2O_3 , for example, the trigonal field is found to reverse in algebraic sign and decrease by one-half.²⁹ Also, the generally accepted placement of the t_0 band below the $t_+ - t_-$ band in metallic V_2O_3 implies a change in the algebraic sign of Δ from that found in $Al_2O_3:V^{3+}$. The fact that $\Delta < \xi$ in V_2O_3 is simply accidental.

Setting $\Delta = 0$, the effect of the spin-orbit coupling alone is to split the ninefold degenerate 3T_1 state into fivefold degenerate $j=2$ manifold, a threefold degenerate $j=1$ manifold, and a nondegenerate $j=0$ state where $\mathbf{j} = \mathbf{l} + \mathbf{s}$. These levels are at $E = 2\xi$ and $E = 3\xi$, respectively. An energy level diagram for V_2O_3 is shown in Fig. 8. A cubic field is expected to lift the degeneracy of the lowest-lying spin-orbit quintet, but this effect will be ignored for the sake of simplicity.

In addition to the external applied magnetic field, orbital and core-polarization hyperfine fields are sensed by the ${}^{51}V$ nucleus, giving rise to the observed Knight shift in the insulating state. Giving careful attention to algebraic signs, the theoretical Knight shift is given by³⁰

$$\Delta H/H = -A \langle \langle s_z \rangle \rangle / H - 2\beta\alpha\kappa \langle \langle l_z \rangle \rangle \langle r^{-3} \rangle / H, \quad (4.3)$$

where the double brackets imply thermal and quantum-mechanical averages. Extrapolating Freeman and Watson's³¹ values from the V^{2+} ion in a sixfold oxygen coordination to V^{3+} , we obtain $A = +170 \text{ kOe}$, $2\beta \langle r^{-3} \rangle = +395 \text{ kOe}$. For both the $j=2$ and the $j=1$ manifold, the Wigner-Eckart theorem gives $\langle l_z \rangle = \langle s_z \rangle = \frac{1}{2} \langle j_z \rangle$ and the Lande g formula give $g = 1.5$ for both states. Using the expression

$$\langle \langle j_z \rangle \rangle / H = j(j+1)g\beta / (3kT), \quad (4.4)$$

we obtain for the thermal average

$$\frac{\Delta H}{H} = - \left(\frac{170 + 395\alpha\kappa}{2} \right) \left(\frac{1.5\beta}{3k(T+\theta)} \right) \times \left[\frac{6 + 2 \exp(-2\xi/kT)}{1 + \exp(-2\xi/kT) + \exp(-3\xi/kT)} \right] \times 10^5, \quad (4.5)$$

where $\Delta H/H$ is expressed in percent, and the paramagnetic Néel temperature θ is added to T as the denominator in Eq. (4.5) by the effect of molecular exchange field.³² Bose *et al.*³³ find $\alpha\kappa = 0.9$ and $\xi = 60 \text{ cm}^{-1}$ from their molecular orbital calculation on hydrated V^{3+} salts, which have very similar g values to vanadium corundum. Based on neutron diffraction data on the low-temperature moment of V_2O_3 , which will be discussed later, we prefer the value $\alpha\kappa = 0.8$ for V_2O_3 , and a corresponding lower value $\xi = 53 \text{ cm}^{-1}$. Equation (4.5) then reads

$$\frac{\Delta H}{H} = - \frac{816}{T+\theta} \frac{6 + 2e^{-152^\circ K/T}}{1 + e^{-152^\circ K/T} + e^{-228^\circ K/T}}, \quad (4.6)$$

where $\Delta H/H$ is expressed in percent Knight shift, and $\theta \approx 600^\circ K$. For $kT \gg \xi$, the expression reduces to $\Delta H/H = -2176/(T+\theta)$, which is to be compared to the experimentally determined temperature-dependent d -band Knight shift of V_2O_3 in the insulating state, $(\Delta H/H)_d = -1323/(T+\theta)$.

The measured Knight shift in the insulating state can be satisfactorily fitted by the empirical expression $\Delta H/H = 1.38 - 1323/(T+\theta)$, a plot of which is included

in Fig. 5. This is to be compared with Jones's complete expression for the metallic-state Knight shift $\Delta H/H = 1.51 - 1643/(T + \theta)$. As in the metallic state, the small value of the Knight shift in the insulating state is caused by the opposing contributions of two large quantities. Comparing the metallic and the insulating states, we find that the values for shifts are comparable, as is anticipated from the use of tight-banding theory.

V. ANTIFERROMAGNETIC STATE

Near 150°K, a phase transformation occurs in V_2O_3 . This transformation is marked by a jump in resistivity of a factor of 10^7 , an abrupt expansion in volume, and the sudden onset of antiferromagnetic order. It is a first-order phase transition, characterized by a hysteresis of about 12°K. Recently Moon⁵ verified the antiferromagnetic ordering of V_2O_3 , using the technique of spin-flip neutron scattering. His measurements show a value for the magnetic moment of $1.2 \mu_B$ per V^{3+} ion. We have already described the abrupt disappearance of the ^{51}V NMR signal at the transition. Shinjo and Kosuge³⁴ performed Mössbauer measurements on Fe-doped V_2O_3 in the temperature range 4.2–300°K. Above $\sim 140^\circ K$, the absorption spectrum was perfectly paramagnetic. Immediately below the transition, a well-resolved six-line splitting appeared, indicative of a large ordered moment. The temperature dependence of the ^{57}Fe internal field, assumed proportional to the temperature dependence of the V^{3+} magnetic moment in pure V_2O_3 , is shown in Fig. 9. An extrapolation of the data indicates an apparent Néel temperature T_N in the vicinity of 200°K.

Bean and Rodbell³⁵ have shown that if the lattice is sufficiently deformable and the exchange constant is a sufficiently sensitive function of lattice strain, the ordering transition will be of first order and a spontaneous distortion of the lattice will occur in the ordered state. If this distortion is large enough to cause the lattice parameter to pass through Mott's critical interatomic spacing, the transition will also be from an itinerant paramagnetic state to a localized antiferromagnetic state. From what has been said previously, we will now show that this appears a quite reasonable explanation for the V_2O_3 M-AF transition.

If we characterize the state of the crystal by a single strain parameter ψ , we may write the free energy

$$\Phi = \frac{1}{2}[B(T) - A(T)]\psi^2 - \lambda[1 - \gamma\psi]M^2 - TS, \quad (5.1)$$

where the first term on the right-hand side is the lattice strain energy, the second term is the magnetic energy (strain-independent plus strain-dependent), and the last is the entropy contribution. $B(T)$ and $A(T)$ are defined in Eq. (3.5) as the phonon and electron-gas contribution to the strain energy, respectively. λ is the magnetic exchange constant, $\gamma = -d\lambda/d\psi$; M is the magnetization. By minimizing the free energy with

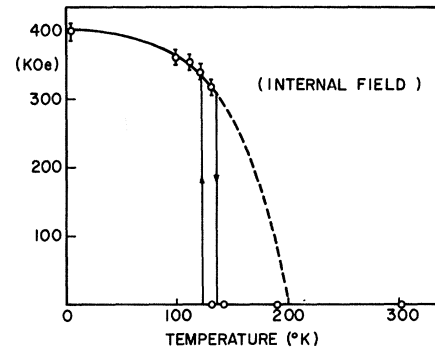


FIG. 9. Temperature dependence of the ^{57}Fe internal field in Fe-doped V_2O_3 (Ref. 34).

respect to both lattice strain and magnetization, Bean and Rodbell obtain

$$M = M_0 \tanh(T/T_N)[1 + (b/3)(M/M_0)^2], \quad (5.2)$$

where $kT_N = \lambda M_0^2/N$ and $b = 3\gamma^2 \lambda M_0^2/[B(T) - A(T)]$. As long as b is less than unity, the transition at the Néel point is second order with the magnetization a continuous function of temperature. But for b slightly larger than unity, the magnetization jumps discontinuously at the Néel point to a finite value. From x-ray studies, McWhan, Rice and Remeika⁸ find that on cooling V_2O_3 through the M-AF transition, both a axes expand while c contracts. The c -axis contraction appears to be magnetostrictive in origin. Since V_2O_3 is on the ragged edge of the M-I transition, the accompanying a -axis expansion produces the enormous low-temperature resistance anomaly by passing through the critical interatomic spacing. The value of b exceeds unity in V_2O_3 because the electron-gas contribution to the strain modulus is almost canceled out by the lattice contribution; i.e., $B(T) - A(T)$ is small at $T \approx 150^\circ K$. When $B(T) - A(T) = 0$, at $T \approx 600^\circ K$, the high-temperature M-I Mott transition occurs.

The critical temperature T_C is related to the apparent magnetic Néel temperature T_N by the formula

$$T_C = T_N(1 - \gamma\psi), \quad (5.3)$$

as shown by Bean and Rodbell. From this relationship, we can derive a value for γ , the strain dependence of the exchange, and see whether the above explanation is a reasonable one. The extrapolated data of Fig. 9 indicate an apparent Néel temperature $T_N = 200^\circ K$, and x-ray diffraction data⁴ yield $\psi = 0.01$. Then

$$\gamma = (1/T_N)[(T_N - T_C)/\psi] = 25. \quad (5.4)$$

This value is to be compared with the value $\gamma = 10.8$ obtained in the same manner by Heeger, Beckman, and Portis³⁶ on the exchange-driven first-order phase transition of $KMnF_3$.

The magnitude of the moment per V^{3+} ion in the

antiferromagnetic phase of V_2O_3 may be deduced from the ground-state wave function described in Sec. IV. The effect of an external magnetic field on the ground-state manifold is shown in Fig. 8. The internal exchange field in the ordered state mimics the effect of an applied external field, but the field splitting is so large that only the lowest-lying sublevel is occupied. This state is given by $|j=2, j_z=+2, l_z=+1, s_z=+1\rangle$ where the z axis of quantization is directed parallel to the observed moment. The value of the magnetic moment

$$\langle M_z \rangle = \mu_B \langle 2s_z - \alpha \kappa l_z \rangle = \mu_B (2 - \alpha \kappa) = 1.2 \mu_B \quad (5.5)$$

is in agreement with the neutron diffraction result. The value for the hyperfine field H_{int} at the ^{51}V nucleus in the low-temperature antiferromagnetic state may be similarly obtained from Eq. (4.3):

$$H_{\text{int}} = [-170 \langle s_z \rangle - 395 \alpha \kappa \langle l_z \rangle] \text{kOe} = -490 \text{kOe}. \quad (5.6)$$

This value for the hyperfine field corresponds to a frequency for resonance $\nu = 550$ MHz. Using a variable frequency NMR spectrometer capable of detecting the naturally abundant ^{53}Cr resonance in antiferromagnet Cr_2O_3 , we have been unable to detect a zero-field NMR signal in V_2O_3 at 4.2°K from 20 to 400 MHz, the limits of the spectrometer. The high value of the hyperfine field predicted by Eq. (5.6) may be responsible for this lack of success.

However, this value for the hyperfine field calculated by assuming $\Delta \approx 0$ is in disagreement with the published experimental value³⁷ of only 175 ± 15 kOe found by inelastic spin-flip scattering. It is possible that the monoclinic distortion associated with the antiferromagnetic phase has quenched the orbital angular momentum and produced the low hyperfine field, but such an explanation is not consistent with a value of $1.2 \mu_B$ for the ordered moment of the vanadium ions. The present author's zero-field NMR investigations have failed to reveal any resonance corresponding to a

hyperfine field anywhere near 175 kOe. The situation surely requires additional experimental investigation.

VI. SUMMARY

Using the technique of nuclear magnetic resonance, we have investigated the metal-insulator transitions in Cr- and Al-doped V_2O_3 . The results of this paper are consistent with the existence of two Mott transitions in this system. We have postulated that the high-temperature phase transition is produced by an instability in a normal vibrational mode of the crystal lattice, and that the low-temperature transition is driven by the large magnetostriction produced by the antiferromagnetic ordering, aided by the presence of this "soft" acoustic-phonon mode. The lattice instability is believed to be caused by the close proximity of a Van Hove singularity to the Fermi energy in the metallic state of the crystal.

This speculative model, based on a band-structure calculation by Nebenzahl and Weger,¹⁸ also explains the anomalous temperature dependence of the Knight shift and the magnetic susceptibility which are observed in V_2O_3 . The rapid variation of the metal-to-insulator Mott transition temperature with impurity doping has its origin in the local change of the stress modulus about the impurity site. The magnitude of the Knight shift in the insulating and metallic states, and that of the local moment in the antiferromagnetic state, has also been treated in this paper.

Note added in proof. Dr. A. C. Gossard has also investigated Cr- and Al-doped V_2O_3 by NMR. His spectra show a smaller temperature range of coexisting insulating and metallic phases than the results presented in the present paper.

ACKNOWLEDGMENTS

The author wishes to thank Dr. E. D. Jones for kindly providing his sample of V_2O_3 crystals, and Dr. J. J. Krebs for many useful discussions.

¹ E. D. Jones, Phys. Rev. **137**, A978 (1964).
² P. H. Carr and S. Foner, J. Appl. Phys. Suppl. **31**, 344 (1960).
³ F. J. Morin, Phys. Rev. Letters **3**, 34 (1959).
⁴ E. P. Warekoi, J. Appl. Phys. Suppl. **31**, 346 (1960).
⁵ R. M. Moon, J. Appl. Phys. **41**, 883 (1970).
⁶ M. Foex et al., J. Rech. Centre Natl. Rech. Sci. Lab. Bellevue (Paris) **4**, 249 (1952); M. Foex and J. Wucher, Compt. Rend. **241**, 184 (1955).
⁷ J. Feinleib and W. Paul, Phys. Rev. **155**, 841 (1967).
⁸ D. B. McWhan, T. M. Rice, and J. P. Remeika, Phys. Rev. Letters **23**, 1384 (1969).
⁹ N. F. Mott, Can. J. Phys. **34**, 1356 (1956), and references therein.
¹⁰ T. M. Rice and D. B. McWhan, IBM J. Res. Develop. (to be published).
¹¹ D. B. McWhan and T. M. Rice, Phys. Rev. Letters **22**, 887 (1969).
¹² Archie J. MacMillan, MIT technical Report No. 172, 1962 (unpublished).

¹³ N. F. Mott, Phil Mag. **6**, 287 (1961).
¹⁴ J. Labbe, Phys. Rev. **158**, 647 (1967).
¹⁵ L. Van Hove, Phys. Rev. **89**, 1189 (1953).
¹⁶ J. Labbe and J. Friedel, J. Phys. Radium **27**, 153 (1966); **27**, 303 (1966); **27**, 708 (1966); Phys. Rev. **158**, 655 (1967).
¹⁷ G. Gilat, Phys. Rev. **157**, 540 (1967).
¹⁸ I. Nebenzahl and M. Weger, Phys. Rev. **184**, 936 (1969).
¹⁹ G. J. Ballhausen, *Introduction to Ligand Field Theory* (McGraw-Hill, New York, 1962), p. 103.
²⁰ W. H. Brumage, C. R. Quade, and C. C. Lin, Phys. Rev. **131**, 949 (1963).
²¹ R. W. Cohen, G. D. Cody, and John J. Halloran, Phys. Rev. Letters **19**, 840 (1967).
²² D. Adler and J. Feinleib, Phys. Rev. Letters **12**, 700 (1964).
²³ W. H. Kleiner, MIT Report No. 3, 1967 (unpublished).
²⁴ J. M. Honig and T. B. Reed, Phys. Rev. **174**, 1020 (1968).
²⁵ D. Adler, J. Feinleib, H. Brooks, and W. Paul, Phys. Rev. **155**, 851 (1967).

²⁶ A. Abragam and M. H. L. Pryce, Proc. Roy. Soc. (London) **A205**, 135 (1951); **A206**, 173 (1951).

²⁷ A. S. Chakravarty, Proc. Phys. Soc. (London) **36**, 711 (1959).

²⁸ J. Umeda, H. Kusumoto, K. Narita, and E. Yamada, J. Chem. Phys. **42**, 1458 (1965); J. Umeda, S. Ashida, H. Kusumoto, and K. Narita, J. Phys. Soc. Japan **21**, 1456 (1966); K. Narita, J. Umeda, and H. Kusumoto, J. Chem. Phys. **44**, 2719 (1966); H. Nagasawa, S. K. Takeshita, and Y. Tomono, J. Phys. Soc. Japan **19**, 764 (1964); S. D. Gornostansky and C. V. Stager, J. Chem. Phys. **46**, 4959 (1967); A. C. Gossard, Phys. Rev. **149**, 246 (1966).

²⁹ J. O. Artman and J. C. Murphy, J. Chem. Phys. **38**, 1544 (1963).

³⁰ A. Okiji and J. Kanamori, J. Phys. Soc. Japan **19**, 908 (1964).

³¹ A. J. Freeman and R. E. Watson, in *Magnetism*, edited by G. T. Rado and H. Suhl (Academic, New York, 1965), Vol. IIA.

³² C. Kittel, *Introduction to Solid State Physics*, 2nd ed. (Wiley, New York, 1956), p. 402.

³³ A. Bose, R. Chatterjee, and R. Rai, Proc. Phys. Soc. **83**, 959 (1964).

³⁴ T. Shinjo and K. Kosuge, J. Phys. Soc. Japan **21**, 2622 (1966).

³⁵ C. P. Bean and D. S. Rodbell, Phys. Rev. **126**, 104 (1962); D. S. Rodbell and C. P. Bean, J. Appl. Phys. Suppl. **33**, 1037 (1961).

³⁶ A. J. Heeger, O. Beckman, and A. M. Portis, Phys. Rev. **123**, 1652 (1961).

³⁷ B. Alefeld, M. Birr, and A. Heidemann, Naturwiss. **56**, 410 (1969).

PHYSICAL REVIEW B

VOLUME 2, NUMBER 12

15 DECEMBER 1970

Phonon Dispersion in Lithium

SATYA PAL

Physics Department, Allahabad University, Allahabad, India

(Received 29 June 1970)

The phonon dispersion relations for lattice waves propagating along the three major symmetry directions of lithium are computed on the basis of the lattice dynamical model of Sharma and Joshi. The calculations are in reasonable agreement with the experimental results of Smith *et al.* obtained from slow-neutron scattering.

The study of lattice vibrations is of fundamental importance in the theory of metals. The past few years have seen the application of powerful new techniques, both theoretical and experimental, to the study of lattice dynamical properties of metals. Because of the complicated nature of the interatomic forces, it is still difficult to work out the lattice dynamics of crystals in an exact way. Thus for a calculation of the properties of solids, it is imperative to resort to various approximate lattice dynamical models—see, for instance, reviews by de Launay,¹ Cochran,² and Joshi and Rajagopal.³ Because of the difficulties involved in developing a theory from first principles, in most of these studies the electronic term in the dynamical matrix is calculated from phenomenological considerations. Essentially, in all these previous studies, attempts have been made to include the effect of conduction electrons in the Born-von Kármán theory of lattice vibrations of solids. Sharma and Joshi⁴ have proposed a semiphenomenological model for the lattice dynamics of cubic metals by considering a central interaction between the nearest and the next nearest ions, and an electron-ion interaction due to the presence of the electron gas. The model has been found to give a plausible explanation of the lattice dynamical behavior of a number of alkali,⁵ noble,⁶ and transition⁷ metals.

Since lithium is, in principle, the simplest of all metals, a knowledge of its lattice dynamics is of importance to any theory of metals. Smith *et al.*⁸ have recently reported the phonon dispersion curves for the lattice waves propagating along the symmetry directions in lithium at 98°K from their experiments on coherent inelastic neutron scattering. The theoretical phonon dispersion curves for lithium have been calculated by the method of pseudopotential.^{9–11} However, in all these calculations the agreement with experiment for most branches is poor.

Krebs's¹² calculations on the basis of the screened Coulomb interaction between the ions embedded in a sea of Bloch electrons are also in poor agreement with the experimental results. In view of the success of the Sharma-Joshi model in cubic metals, it was thought worthwhile to reconsider the theoretical side of lattice vibrations in lithium on the basis of this model.

The phonon dispersion curves for lithium for the lattice waves propagating along the symmetry directions $[\xi 0 0]$, $[\xi \xi 0]$, and $[\xi \xi \xi]$ are computed from the dispersion relations for a bcc metal.⁴ The calculated dispersion curves are shown in Fig. 1, where for comparison the experimental points of Smith *et al.* have also been plotted. The force constants have been estimated from the experimental values of the elastic